

Extension of the drag coefficient function for a stationary sphere on a boundary of similar spheres

Neil L. Coleman

Supervisory Geologist, USDA Sedimentation Laboratory, Oxford, MS, USA

Introduction

Scaled-up Reynolds models, in which large bodies simulate small particles, are used to study erosive forces acting on individual streambed particles, because these forces cannot be studied by conventional flume experiments or in the field. In current practice, spheres represent the streambed particles in the model, so that effects of secondary variables, like particle shape and orientation, are removed. Aksoy [1] has remarked that these simplified models can demonstrate basic physical principles, but that they cannot provide results that can be applied directly to natural streambed particles. One basic physical principle that lends itself well to model study is the nature of the drag coefficient function for a streambed particle. Furthermore, since streambed particles are usually close to spherical in shape, the results of the model study may be more directly applicable than Aksoy has supposed.

Coleman [2] produced experimental evidence indicating that, for Reynolds numbers from about 70 to 10,000 the drag coefficient function for a stationary sphere resting on a bed of closely packed identical spheres resembled that for a sphere falling in an infinite fluid. This finding contrasted with evidence produced by Garde and Sethuraman [3], showing that the drag coefficient function for a sphere rolling on a bed of spheres was higher than the function for a sphere in free fall. The latter result was obtained for Reynolds numbers from 0.1 to 10,000. Figure 1, from the 1972 report of Coleman [2] compared the functions for the rolling and stationary spheres, to the extent that they could be compared at that time. No comparison could be made for Reynolds numbers below 70.

Recent development of an improved research facility has allowed stationary sphere drag experiments

to be performed over a range of Reynolds numbers from 0.4 to 10,000, which extends the drag coefficient function to a range of lower Reynolds numbers than those covered in Coleman's earlier [2] work. The results from these experiments are presented here to extend the comparison of drag coefficient functions over the attainable Reynolds number range.

Apparatus

The improved research facility used for these experiments consisted of a recirculating closed system water tunnel driven by a variable speed pump with a maximum capacity of 0.078 m³/s. The water tunnel has a rectangular conduit 10.16 m long with a test section 0.27 m wide by 0.18 m high. For these experiments, a bed of plastic spheres 13 mm in diameter was glued to the floor of the conduit, with its leading edge 7.38 m from the conduit entrance. The isolated sphere for drag force measurements was located on the centerline of the bed, 1.1 m from the leading edge. It was attached to a drag force transducer. This transducer was of the strain gauge load beam type, similar to that used in earlier work [2], and to that used by Aksoy [1]. However, it had the added feature that the velocity of flow approaching the test sphere could be measured by sensing the stagnation pressure at a piezometer hole in the sphere front, so that approach flow velocity and drag force on the sphere were measured simultaneously. The piezometer hole in the sphere was connected to a commercial differential pressure transducer, and referenced to a second piezometer tap in the water tunnel wall.

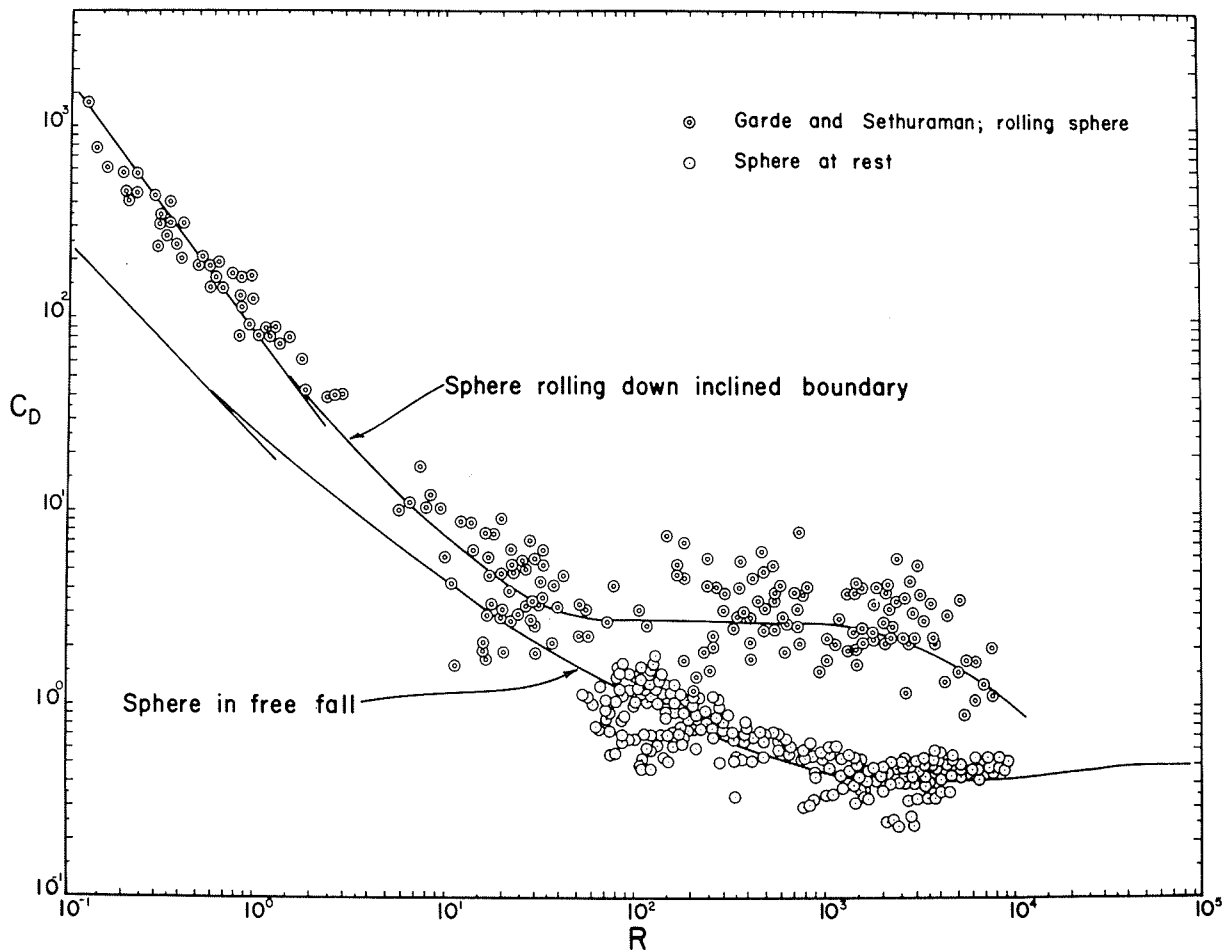


Figure 1. — Comparison of drag coefficients for rolling sphere, stationary sphere, and falling sphere. After Coleman [2].

Both the strain gauge bridge for force measurement and the differential pressure transducer for velocity measurement were excited by appropriate carrier preamplifiers, and additional readout amplification was provided for measuring small forces and velocities. Output was recorded with a multiple channel high-speed millimeter recorder.

The equipment was operated with water, or with solutions of hydroxyethylcellulose (HEC) in water. The polymer HEC when dissolved in water, provides working fluids whose viscosities can be varied and which are superior in stability, Newtonian behavior, and ease of mixing, to the solutions of sodium carboxymethylcellulose used previously [2]. Kinematic viscosities ranging from 9.30×10^{-7} to 1.13×10^{-3} m²/s were obtained using HEC solutions. By using these solutions and by varying the discharge in the water tunnel, the experimental range of sphere Reynolds numbers from about 0.4 to 10,000 was obtained.

Procedures

At the beginning of the experiments, the water tunnel was filled with a HEC solution of 3% concentration, with a viscosity of 1.13×10^{-3} m²/s. After

a series of experiments was completed with this fluid, a new fluid was produced by diluting the original solution with an arbitrary volume of water. The dilution process was repeated to produce 17 different working fluids; the final fluid was water with no HEC. Temperature-viscosity curves for each fluid were obtained by withdrawing a sample from the water tunnel and analysing it with a falling ball viscosimeter in a controlled temperature bath. Densities were measured by weighing a known volume of the sample.

Each experiment consisted of operating the water tunnel at a selected flow rate, observing the temperature by means of a thermometer inserted through the conduit wall, and then simultaneously recording the outputs of the velocity and force measuring systems. Each series of experiments consisted of tests at three to six different flow rates (approach flow velocities) with each test repeated twice. Recording times for approach flow velocity and drag force varied from 30 s to 2 mins, depending on the observed intensity of flow turbulence and force fluctuation.

Between each set of experiments, the drag force strain gauge bridge was calibrated against a balance specially built for the purpose, and the differential pressure transducer in the velocity measuring system was calibrated against a water manometer.

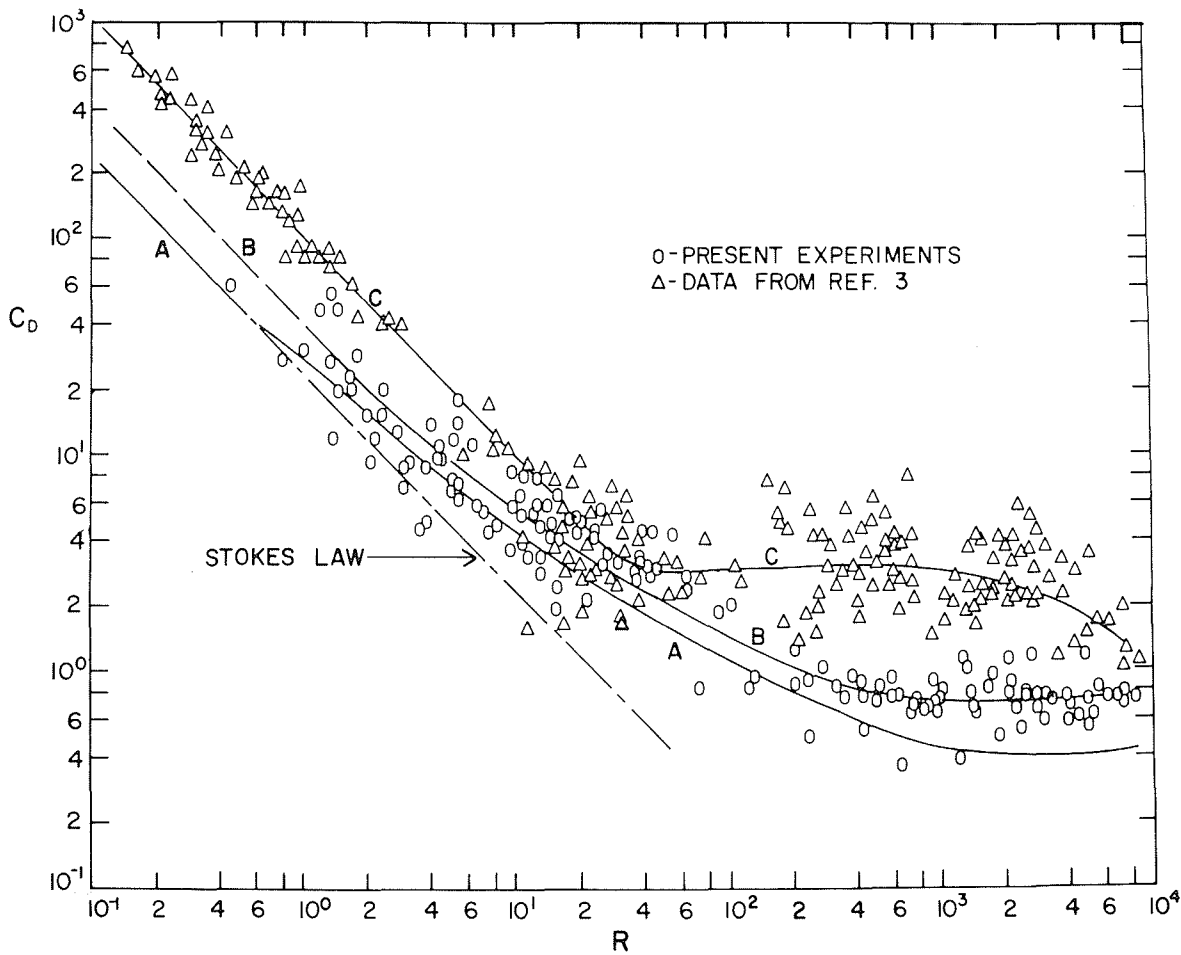


Figure 2. — Comparison of stationary sphere drag coefficients from this experiment with drag coefficients for a rolling sphere and a falling sphere.

Analysis

The recorded outputs of the measuring systems were integrated to obtain time-averaged output values. The time-mean drag force f could then be read directly from the force transducer calibration curve. For the velocity-measuring system, the time-mean output I of the pressure transducer was related to the dynamic head at the front of the sphere by:

$$I = 0.47 h \tag{1}$$

where h is the head (in meters). The velocity U could then be calculated from:

$$U = \left(\frac{2g}{0.47} \frac{I}{P} \right)^{1/2} \tag{2}$$

where g is the gravity field strength, and P is the pressure coefficient of Homann [4] for a sphere in viscous flow:

$$P = 1 + \frac{6}{0.5R + 0.32(R)^{1/2}} \tag{3}$$

With experimental values of f and U , the drag coefficient C_D and the Reynolds number R are calculated from:

$$C_D = \frac{8f}{\pi D^2 \rho U^2} \tag{4}$$

and

$$R = \frac{UD}{\nu} \tag{5}$$

where D is the sphere diameter, and ρ and ν are the fluid density and kinematic viscosity, respectively.

Results

Figure 2 shows the present results, as compared with those of Garde and Sethuraman [2] for a rolling sphere. Of the three curves, curve A is the classical curve for a sphere in free fall; B is a tentative curve of best visual fit to the present data; and C is a curve of best visual fit to the rolling sphere data.

Unlike the data in Figure 1, the data from these experiments formed a curve (*B*) somewhat greater than the classical drag curve (*A*), at least for high Reynolds numbers. For low Reynolds numbers, data scatter prevented any firm conclusion as to whether curve *B* approached the standard curve, or paralleled it. Nevertheless, curve *B* was substantially lower than curve *C* for a rolling sphere. As is well known, for $R < 1$ the classical drag curve corresponds to Stokes' law:

$$f = 3\pi D\rho\nu U \quad \text{or} \quad C_D = \frac{24}{R} \quad (6)$$

Similarly, the rolling sphere data (Curve *C*) conformed very well, for $R < 20$, to a Stokes-type law:

$$f = 12.5\pi D\rho\nu U \quad \text{or} \quad C_D = \frac{100}{R} \quad (7)$$

If the stationary sphere data from the present experiments approached curve *B* as drawn for $R < 3$, then the speculation arises that, for a sphere resting on a bed, a Stokes-type law would apply with the form:

$$f = 5\pi D\rho\nu U \quad \text{or} \quad C_D = \frac{40}{R} \quad (8)$$

Conclusions

Experimental drag coefficients for a sphere resting on a bed were determined. These drag coefficients formed a function that was generally lower than that for a sphere rolling on a bed. The data from the experiments described here, together with the rolling sphere data of other workers, give rise to the speculation that a Stokes-type law would apply for stationary and rolling spheres on a bed, where numerical coefficients are 5 and 12.5 for the stationary and rolling spheres, respectively, as compared with the numerical coefficient of 3 in Stokes' law for a sphere in free fall.

References

- [1] AKSOY S. – Fluid force acting on a sphere near a solid boundary. Proc. 15th Congress, IAHR, Istanbul, 1973, p. 217-224.
- [2] COLEMAN N.L. – The drag coefficient of a stationary sphere on a boundary of similar spheres. *La Houille Blanche*, No. 1, 1972, p. 17-21.
- [3] GARDE R.J. and SETHURAMAN. – Variation of the drag coefficient of a sphere rolling along a boundary. *La Houille Blanche*, No. 7, 1969, p. 727-732.
- [4] HOMANN F. – The effect of high viscosity on the flow around a cylinder and a sphere. *NACA Tech. Mem. 1334*, June, 1952, 62 p.